Paper

PREDICTIONS OF DISPERSION AND DEPOSITION OF FALLOUT FROM NUCLEAR TESTING USING THE NOAA-HYSPLIT METEOROLOGICAL MODEL

Brian E. Moroz,* Harold L. Beck,† André Bouville,* and Steven L. Simon*

Abstract—**The NOAA Hybrid Single-Particle Lagrangian Integrated Trajectory Model (HYSPLIT) was evaluated as a research tool to simulate the dispersion and deposition of radioactive fallout from nuclear tests. Model-based estimates of fallout can be valuable for use in the reconstruction of past exposures from nuclear testing, particularly where little historical fallout monitoring data are available. The ability to make reliable predictions about fallout deposition could also have significant importance for nuclear events in the future. We evaluated the accuracy of the HYSPLIT-predicted geographic patterns of deposition by comparing those predictions against known deposition patterns following specific nuclear tests with an emphasis on nuclear weapons tests conducted in the Marshall Islands. We evaluated the ability of the computer code to quantitatively predict the proportion of fallout particles of specific sizes deposited at specific locations as well as their time of transport. In our simulations of fallout from past nuclear tests, historical meteorological data were used from a reanalysis conducted jointly by the National Centers for Environmental Prediction (NCEP) and the National Center for Atmospheric Research (NCAR). We used a systematic approach in testing the HYSPLIT model by simulating the release of a range of particle sizes from a range of altitudes and evaluating the number and location of particles deposited. Our findings suggest that the quantity and quality of meteorological data are the most important factors for accurate fallout predictions and that, when satisfactory meteorological input data are used, HYSPLIT can produce relatively accurate deposition patterns and fallout arrival times. Furthermore, when no other measurement data are available, HYSPLIT can be used to indicate whether or not fallout might have occurred at a given location and provide, at minimum, crude quantitative estimates of the magnitude of the deposited activity. A variety of simulations of the deposition of fallout from atmospheric nuclear tests conducted in the Marshall Islands (mid-Pacific), at the Nevada Test Site (U.S.), and at the Semipalatinsk Nuclear Test Site (Kazakhstan) were performed. The results of the Marshall Islands simulations were used in a limited fashion to support the dose reconstruction described in companion papers within this volume. Health Phys. 99(2):252–269; 2010**

Key words: Marshall Islands; nuclear weapons; fallout; modeling, meteorological

INTRODUCTION

COMPUTER MODELS have been both influential and beneficial in predicting fallout dispersion and deposition. These models have been used historically for such diverse tasks as producing quick fallout estimates necessary for immediate health assessments, extending exposure estimates downwind beyond ground-based measurements in retrospective dose and risk assessments (Cederwall and Peterson 1990; Hoecker and Machta 1990), and projecting potential physical damage, including atmospheric effects such as smoke production from regional nuclear conflicts and individual acts of nuclear terrorism (Toon et al. 2007). Computer codes used for such purposes were developed and applied by the scientific and defense communities as early as the 1960's (Rowland 1994).

Modeling the transport and deposition of particles released from a nuclear weapons test is both a complex and highly uncertain exercise. This is true even when the meteorological data used in the simulation are accurate. Furthermore, in order to simulate the deposition density of specific radionuclides or total radioactivity, a model is required for the spatial distribution of radionuclides in the initial debris cloud as well as the distribution of activity as a function of particle size. The most computationally burdensome factors in performing the simulations are the large size of the debris cloud and, therefore, the large number of particles and particle sizes that are needed to conduct a realistic fallout simulation over long distances. An additional difficulty is presented when modeling wet removal processes. Both in-cloud and below-cloud wet removal processes may be of great importance to accurately simulating deposition when precipitation occurred downwind. The data available

* Division of Cancer Epidemiology and Genetics, National Institutes of Health, National Cancer Institute, Bethesda, MD, 20892; † New York, NY.

For correspondence contact: Steven L. Simon, National Cancer Institute, National Institutes of Health, 6120 Executive Blvd., Bethesda, MD 20892, or email at ssimon@mail.nih.gov.

(*Manuscript accepted* 22 *June* 2009)
0017-9078/10/0

DOI: 10.1097/HP.0b013e3181b43697

from most meteorological archives are generally insufficient for accurately modeling these processes (Draxler and Hess 1997, 1998). Therefore, simplifying assumptions are usually incorporated into wet removal algorithms, leading to predictions with low reliability.

Given the present national security concerns, there is a need for the scientific and defense communities to be aware of the capabilities of available atmospheric transport models and their possible application to predict fallout in the case of future events. This paper discusses one particle transport and dispersion model, the Hybrid Single-Particle Integrated Trajectory (HYSPLIT) model, and describes how the model was tested and evaluated for the purpose of reconstructing fallout resulting from nuclear testing. Our main evaluation was of U.S. nuclear tests conducted in the Marshall Islands (MI). In addition to the Marshall Islands nuclear tests, two other fallout events were simulated to test the model: the 1953 Upshot-Knothole Harry test at the Nevada Test Site (NTS) and the first Soviet nuclear test conducted at the Semipalatinsk Test Site in 1949. In a latter section of this paper, we discuss one application of the HYSPLIT model: our use of the model to support deposition and dose estimates in the Marshall Islands reported in companion papers (Beck et al. 2010; Bouville et al. 2010; Simon et al. 2010a, 2010b). Based on the test simulations and the application mentioned above, the potential use of HYSPLIT predictions for both past and future fallout events is discussed.

MATERIALS AND METHODS

The HYSPLIT model

HYSPLIT (Draxler and Hess 1997, 1998; Draxler 1999) was developed and is maintained by the National Oceanic and Atmospheric Administration Air Resources Laboratory (NOAA ARL). The HYSPLIT model computes the dispersion and deposition of particles originating from single or multiple source locations upon a simultaneous release. In this paper, HYSPLIT was used to simulate the advection and dispersion of particles in a radioactive debris cloud over the time period of several hours to several days following the nuclear test. Here we recognize that HYSPLIT was not developed as a predictive fallout model; it makes no attempt to simulate the dynamics of the debris cloud prior to stabilization, nor does it simulate the radioactivity associated with a particular particle size. However, by assuming the debris cloud is stabilized, and assuming reasonable distribution of particles and particle sizes within the stabilized cloud, multiple simulations of the transport of particles released at various altitudes, for a range of particle sizes, can be combined to approximate the total fallout deposited from a debris cloud as the particles from each altitude are transported downwind.

Meteorological input data used by HYSPLIT are gridded meteorological data fields generated and archived from other meteorological models, although it is possible to perform simulations with user-defined wind data to a limited extent (Draxler and Hess 1997, 1998; Draxler 1999). Because it is common for different meteorological models to use different vertical coordinate systems, HYSPLIT linearly interpolates the meteorological data at each horizontal grid point in the meteorological input data to an internal sub-grid containing a terrain-following coordinate system where all heights are expressed relative to mean sea level (Draxler and Hess 1997, 1998). The default vertical resolution for HYSPLIT defines the model's lowest level (level 1) at approximately 10 m and level 2, which is considered the surface layer, at approximately 75 m above ground level (AGL). Vertical resolution continually decreases away from the ground surface following a quadratic form. It is possible to modify the model's internal vertical resolution by modifying the internal parameters corresponding to the model's internal height index (Draxler and Hess 1997). In contrast, the horizontal resolution applied by the model is equivalent to the horizontal resolution of the meteorological input data.

The spacing between the grid points of the input data influences the accuracy of model computations. As a general rule, the grid resolution should, at minimum, correspond to the scale and the purpose of the simulation. Data gridded at a coarse resolution may yield less precise results than desired. In contrast, finely gridded data can improve model results, assuming that the meteorological input data are accurate. The small amount of gridded meteorological data at fine resolutions in the tropic zones of the Pacific during the period of U.S. nuclear testing in the Marshall Islands was one limiting factor to our work.

HYSPLIT offers several particle or puff modeling approaches which are discussed in Draxler and Hess (1997, 1998). We used the three-dimensional particle model to compute the advection and dispersion of the debris cloud. Advection is computed independently, or prior to, the dispersion calculation. The dispersion rate is dependent upon the vertical diffusivity profile, wind shear, and the horizontal deformation of the wind field (Draxler and Hess 1997).

The particle advection algorithm has two primary steps. After linearly interpolating the velocity vectors (u, v, w) to the current particle position and time, a displacement calculation yields a first-guess position by integrating the velocity component at the current position and time over the duration of the time-step. The final position is then calculated by averaging the velocity components

at the two successive particle positions, integrating over the duration of the time-step, and then adding the displacement to the initial position of the particle. The integration time-step can vary from 1 to 60 min but is bound by a user-specified advection distance per time-step to limit the advection to less than one grid point per time-step.

Dispersion is computed after the advection computation; however, it is necessary for the model to first compute stability and mixing coefficients. Stability and mixing are estimated from the meteorological input data. Heat and momentum fluxes, if they are present in the meteorological data, are used to compute the stability, otherwise temperature and wind data at each grid point are used to estimate it. Vertical mixing within the boundary layer is computed as an average at each horizontal grid point based upon flux data. Above the boundary layer, vertical mixing is estimated from the wind and temperature profiles. Horizontal mixing is computed using the deformations in the wind field and is adjusted based on the size of the meteorological grid.

To realistically simulate the dispersive nature of the atmosphere, a random turbulent component is incorporated into the dispersion calculation by adding the turbulent component to the mean velocity obtained from the meteorological input data at each time-step. This turbulent component is a Gaussian based *pseudo*-randomly generated number resulting from the product of the Gaussian random number and the standard deviation of the computed turbulent velocity of the velocity vector (Draxler and Hess 1997). The Gaussian random number is generated using a variation of the linear congruential method, $X_{i+1} = (aX_i + c)\ mod\ m$, where the element i indicates the position of the random number within the sequence. When the parameters a, c, and m are chosen correctly, generators of this class can ensure a nonrepeating sequence on the scale of 10^9. It should be noted that though the HYSPLIT model incorporates a random turbulence element, the model is not stochastic because the same random sequence is generated with each invocation of the model, meaning that the model results for any single simulation will always be the same assuming the simulation parameters are not changed. This can be altered by simply modifying the model's random number algorithm to apply a different seed value with each invocation.

Several dry deposition options are available to the model user. In our case, dry deposition was simulated under the assumption that the deposition velocity for all particles was equivalent to the gravitational settling velocity. For local fallout from weapons tests, this is a reasonable approximation since most of the radioactivity is found on particles of diameter greater than 5 μm (Heidt et al. 1953; Crocker et al. 1965; Ibrahim et al. 2010). Other HYSPLIT options include implicitly specifying a dry deposition velocity or using the resistance method (Draxler and Hess 1997). In our simulations, gravitational settling was computed by the model based on particle diameter, a fixed particle density of 2.5 g cm^{-3}, and a fixed spherical particle shape. The computed settling velocity is applied to the vertical position of the particle at each time-step. Particles are subject to dry deposition removal processes upon entering the model's surface layer. The model computes dry deposition using one of two options: either removing a fraction of the particle's mass over successive time-steps until the mass becomes zero, or computing the probability that a particle will deposit all of its mass during a single time-step (Draxler and Hess 1997). In our simulations the deposition probability option was used.

Wet deposition processes impose difficulties in meteorological computer models. The difficulty stems from the simplified assumptions incorporated into wet deposition models coupled with a general lack of reliable precipitation observations in the meteorological input data (Draxler and Hess 1997). Both in-cloud (rainout) and below-cloud (washout) wet deposition are estimated in the HYSPLIT model by defining the fraction of total pollutant mass within and below the cloud layer and applying an estimated deposition rate. The extent of the cloud layer is defined using relative humidity (RH) in the meteorological profile at each horizontal grid point. The cloud top and bottom are, by default, defined at 60% and 80% RH, respectively. In the case of rainout, a wet deposition velocity is calculated as the product of the precipitation rate at the grid point and a pollutant-specific scavenging ratio. The scavenging ratio is based on the amount of pollutant (g L^{-1}) in the air within the cloud to that in the rain (g L^{-1}) measured on the ground at the grid point (Draxler 1999). The wet deposition velocity is then applied to the fraction of pollutant mass within the cloud layer. Below-cloud removal is defined using only a rate constant (s^{-1}) and is independent of precipitation rate (Draxler and Hess 1997). The rate constant is applied to the fraction of pollutant that is below the cloud bottom. In our simulations, the model's default values for the in-cloud scavenging ratio (3.2×10^5 L per L) and the below-cloud rate constant (5.0×10^{-5} s^{-1}) for wet deposition processes were used.

The total deposition over a time-step is the sum of the removal amounts resuting from each process. The total pollutant mass is then reduced by the computed removal fraction (Draxler and Hess 1997).

Several verification examples demonstrating the applicability and accuracy of HYSPLIT computations in the areas of particle advection, dispersion, and deposition

are provided in Draxler and Hess (1998). Draxler and Hess (1998) discussed a HYSPLIT simulation of the release from the Chernobyl reactor accident which took place in the former Soviet Union in 1986. Resulting deposition contours and peaks were compared against those reported in Klug et al. (1992). It was found that contour patterns were reasonably consistent and the HYSPLIT-computed deposition peaks were numerically ~10% higher than the reported values in the best case. Two additional studies which used HYSPLIT as a research tool for modeling fallout processes include Kinser (2001) and Swanberg and Hoffert (2001), who simulated releases of ^{137}Cs from the Chernobyl reactor accident to investigate model-predicted wet deposition and resuspension as a source of ^{137}Cs in Europe.

Meteorological input data

High spatial density meteorological data are either not available or are very sparse during the 1950's for many areas including the mid-Pacific Ocean where the Marshall Islands are located, the NTS, and the Semipalatinsk Test Site. For that reason, meteorological input data from a reanalysis data set were used. The reanalysis was conducted as a collaborative effort between the National Centers for Environmental Prediction (NCEP) and the National Center for Atmospheric Research (NCAR) with the purpose of recovering historical weather observations from many sources, providing quality control of the data, and compiling the results so as to fulfill the research needs for climate monitoring and prediction. The NCEP/NCAR database covers the period 1948–2008 and provides forecasts at regular temporal intervals of four times daily (though, during the period 1948–1957, forecasts are provided eight times daily) and at a spatial resolution of 2.5 degrees.

The most important observational data incorporated into the reanalysis data set for the purposes of our study are the upper-air wind data. Upper-air wind data are primarily derived from the world's upper-air rawinsonde network, although a considerable amount of aircraft reconnaissance data was also incorporated into the NCAR/NCEP reanalysis. The U.S. Air Force prepared a global collection of aircraft data that covered the time period 1948–1970. Aircraft data were also contributed by the University of Hawaii from locations in the tropics for the time period 1960–1973.

Early rawinsonde coverage in the U.S. is fairly complete, though less data are available for other parts of the world. Good coverage in the U.S. began in 1948 while periods of good coverage in China, India, and Russia cannot be found earlier than the 1950's and 1960's. Wind profiles from several operational weather stations in the Marshall Islands were available in addition to upper-air wind measurements taken at test site locations by the U.S. Army (DNA 1979), although the supporting literature does not unequivocally report that those observations were incorporated into the NCAR/NCEP reanalysis.

Precipitation observations in the reanalysis data set are also important, but appear to be much less reliable than upper-air wind data. In the NCAR/NCEP reanalysis model, observed precipitation data do not play a direct part in the reanalysis output. Precipitation data are solely driven by the reanalysis model and can exhibit regional biases (Kalnay et al. 1996).

NUCLEAR TEST SIMULATIONS AND MODEL EVALUATIONS

General methods

The HYSPLIT model was tested using a systematic approach for simulating the transport and deposition of radioactive particles resulting from a nuclear weapons test. A range of particle sizes were released from a range of altitudes at a single source location and tracked over time. The proportion of deposited particles and the location of deposition were then evaluated by comparing model-predicted deposition patterns and time of fallout arrival against known deposition patterns and best available estimates.

In order to simulate the deposition density of a specific radionuclide, such as ^{137}Cs, a crude model was developed to qualitatively relate HYSPLIT particle deposition to ^{137}Cs deposition as a function of fission yield, debris cloud size, and stabilization altitude. This model assumes a lognormal distribution of activity as a function of particle diameter based on data from the NTS (Izrael 2002). In order to simulate ^{137}Cs ground deposition density (Bq m^{-2}) for comparison with the ^{137}Cs deposition densities in the Marshall Islands reported by Beck et al. (2010), the ^{137}Cs particle-size distribution was modified to reflect the fact that ^{137}Cs tends to be depleted on larger particles. Much of the ^{137}Cs is formed after the heavier particles have already deposited due to ^{137}Cs having a gaseous precursor, ^{137}Xe (Beck et al. 2010). Here we assume that ~80% of the total ^{137}Cs activity is found on particles less than 50 μm in diameter. This assumption is consistent with data and models for a coral surface shot, as reported by Freiling et al. (1965). The apportionment of the ^{137}Cs on particle sizes less than 50 μm (i.e., 80%) was chosen based on experience and judgment since little actual data are available from the literature. The particle-size distributions for ^{137}Cs activity used for the Marshall Island simulations are shown in Table 1. In order to estimate the sensitivity of the simulated deposition density of ^{137}Cs, two other particle-size distributions were tested in selected simulations. The

Table 1. Estimated distribution of ^{137}Cs activity on particles of specified diameters.

Median particle diameter, μm (range)	Activity (%) of total		
	MI ^{137}Cs distribution	Alternate ^{137}Cs distribution #1	Alternate ^{137}Cs distribution #2
5 (2.5–7.5)	12.5	16.6	23.6
10 (7.5–12.5)	11.0	11.6	11.7
15 (12.5–17.5)	10.0	9.3	7.5
20 (17.5–22.5)	9.0	8.1	5.3
25 (22.5–27.5)	8.0	6.9	3.9
30 (27.5–32.5)	7.0	6.2	3.0
35 (32.5–37.5)	6.5	5.4	2.4
40 (37.5–42.5)	6.0	5.0	2.0
45 (42.5–47.5)	5.5	4.4	1.6
50 (47.5–52.5)	5.0	3.7	1.4
55 (52.5–57.5)	4.5	3.3	1.2
60 (57.5–62.5)	4.0	2.9	1.0
65 (62.5–67.5)	3.5	2.6	0.9
70 (67.5–72.5)	2.5	2.3	0.8
75 (72.5–77.5)	1.8	2.0	0.7
80 (77.5–82.5)	1.2	1.8	0.6
85 (82.5–87.5)	0.9	1.5	0.6
90 (87.5–92.5)	0.7	1.4	0.5
95 (92.5–97.5)	0.3	1.2	0.5
100+	$\leq$0.1	$\leq$1.0	$<$1.0

two alternative distributions, also shown in Table 1, varied the fraction of ^{137}Cs on particles greater than 50 μm slightly from the distribution labeled MI.

The distribution of activity and of the number of particles within the stem and the assumed spherical head of the nuclear debris cloud were based on assumptions from previous publications on meteorological modeling of nuclear debris clouds. Here, we assumed that 12% of the activity was deposited in the stem as derived from data on NTS nuclear test debris clouds (Hoecker and Machta 1990; NCI 1997). The remaining 88% of the activity was assumed to be distributed homogenously throughout the head of the cloud as well as the number of particles in each size fraction. Another simplifying assumption made for the simulations was to release all particles from the vertical axis through the center of the spherical head of the debris cloud.

The total amount of ^{137}Cs in the debris cloud was calculated from the estimated fission yield of each test. Note that the fission yields used for normalization are only estimates, since the fission yields for U.S. thermonuclear tests remain classified. The ^{137}Cs activity for each particle tracked by the model was based on the total ^{137}Cs produced and its apportionment among the total number of particles using the distributions of activity as a function of particle diameter (Table 1).

The debris cloud model used in these simulations is acknowledged to be crude; hence, the fallout estimates are subject to a large degree of uncertainty. More sophisticated simulations of the distribution of activity in the cloud and on various sized particles have been done in other studies (see for example, Cederwall and Peterson 1990). However, since the particle-size and activity distributions can vary significantly with the particular conditions of a test such as height of burst, type of soil, and yield (see companion paper by Ibrahim et al. 2010), even simulations using more elaborate models (Cederwall and Peterson 1990) were forced to adjust the activity, altitude, and particle size parameter estimates for each test to achieve even marginal agreement with actual measurements.

Once a particle is deposited in a HYSPLIT simulation, its location relative to points of interest has to be determined. For that purpose, we defined rectangular areas (termed "deposition domains") in which the deposition density of particles and activity were determined by counting the number of deposited particles stratified by release height and diameter. Each domain was defined by the longitude and latitude of two points on opposing corners. The coordinates of each deposited particle could be tested to determine if the particle had deposited within the domain bounded by the defined rectangle.

Marshall Islands nuclear tests

The HYSPLIT model was tested by simulating fallout deposition from selected U.S. nuclear tests conducted at the Bikini and Enewetak test sites in the Marshall Islands. Model-predicted deposition patterns, density estimates, and fallout time of arrival were compared against patterns and values reported in the literature (see Beck et al. 2010 for a listing of available data).

The large area of the Marshall Islands imposed significant computational constraints because it is necessary to simulate very large numbers of particles in order to delineate spatial or temporal patterns with satisfactory reliability. Using a three-dimensional particle dispersion model, the number of particles required for reasonably precise simulations of multi-day fallout dispersion from an entire debris cloud was too large to be practically followed in a single HYSPLIT simulation. Thus, smaller simulations were performed, each for a single release altitude and particle size. In each of these simulations, 10,000 particles were released. The results of the simulations were then combined based on the assumed relative fractions of total ^{137}Cs activity released from various portions of the debris cloud and the fraction of activity released from various altitudes as discussed above. For the individual altitude and particle size combinations, release heights were varied from ground level to the reported top of the radioactive debris cloud (DNA 1979) in 1,000 m increments. The particle sizes simulated ranged from 1 to 100 μm in 5 μm increments and from 125 to 300 μm in 25 μm increments and were selected based on the typical range of particle sizes for weapons

debris reported in many publications (see Ibrahim et al. 2010).

The fallout arrival time was assessed by calculating the time for various particle sizes released from each altitude to be deposited in specific deposition domains used to define specific atolls in the Marshall Islands. Three separate deposition domain sizes were used to estimate average deposition density (Bq m^{-2}) for the region surrounding an atoll. As an approximation of the land area encompassed by an atoll, each atoll area was approximated by a deposition domain defined by the most extreme point of each atoll's boundaries in north, south, east and west directions. To account for possible prediction error resulting from inadequate meteorological data or due to the statistical limitations imposed by simulating too few particles, a larger domain was also defined by increasing the size of the original domain by an additional 50% in both longitude and latitude. In the case of very small atolls, increasing the domain size using the method just described did not make a significant difference in the number of particles counted. For that reason, a third domain size, measuring 1 square degree, was also used in simulations. For large atolls such as Kwajalein, the areas represented by the 1 square degree domain and the smaller rectangular areas were not greatly different. By comparing the estimated deposition density averaged within each of the three different domains, we could assess the sensitivity of the estimated deposition density to small spatial variations in particle trajectories, as well as the precision of the deposition density estimates since, for the smaller atolls, the deposited fraction of the 10,000 particle source term was often very small. Thus, the precision of estimates based on the smaller domains was often poor.

In addition to the primary particle size-activity distribution (labeled MI in Table 1), two alternative distributions were also used in the Castle Bravo simulation to investigate the sensitivity of the ^{137}Cs deposition density estimates to the assumed size-activity distribution. Because most of the atolls of interest were at large distances (hundreds of kilometers) from the Bikini Atoll test site, the deposited particles were mostly less than 50 μm in diameter; thus, the estimated ^{137}Cs deposition densities for most atolls were not highly sensitive to the assumed particle size-activity distribution.

The estimated deposition density of ^{137}Cs at any atoll will be sensitive to the assumed spatial distribution of activity in the cloud, particularly, the spatial distribution of the smaller particles that carried most of the ^{137}Cs. However, as discussed earlier, the actual spatial distribution of activity in the cloud probably varies with the location, yield, and conditions of the test. For this reason, errors in the exact meteorology tended to have a much larger impact on the estimated deposition at a specific atoll than did assumptions inherent in the debris cloud model, resulting in (1) simulations failing to predict fallout at an atoll when it was known to actually have occurred, and (2) predicting fallout arrival times that were much later than the reported or assumed arrival time.

In order to estimate the relative impact of the HYSPLIT wet deposition model on the predicted fallout deposition, each simulation was run twice, once with precipitation processing enabled and once with precipitation processing disabled.

General results. Predicting deposition density (Bq m^{-2}), usually of ^{137}Cs, was of potential use in assessments of radiation doses in the Marshall Islands (Beck et al. 2010; Bouville et al. 2010; Simon et al. 2010a, 2010b). However, evaluating the accuracy of the simulations of deposition density for the Marshall Islands tests was hindered by the absence of a large and consistent set of empirical ground measurements of radioactivity following individual nuclear tests as well as accurate meteorological data. The reliability of trajectories in close proximity to the test site could be inferred from comparisons between observed wind data at the test site, and the initial wind speed and direction used by the model. The HYSPLIT-interpolated wind data resulting from the meteorological input data sets used in simulations were compared with the actual wind speed and direction at many different altitudes reported from measurements at the test sites (DNA 1979). Direct observations of wind speed and direction as a function of altitude downwind from the test sites were not available except for a few tests, and in those cases, the observations were available at only one location downwind. For these reasons, no other systematic comparisons of wind speed and direction could be made. In general, the agreement between HYSPLIT simulated deposition and available measurement data tended to be much better when the initial wind speed and direction from the meteorological reanalysis data (interpolated by HYSPLIT) were similar to that measured at the test atoll at the time of the test.

Because our assumptions used to estimate activity per particle were crude, and because the meteorological input data had limited accuracy, the HYSPLIT simulations could only yield estimates of deposition density with significant uncertainty. Even determining whether or not any fallout had even occurred was often difficult given the generally coarse resolution of the meteorological input data. Our findings indicate that even a relatively small error in wind direction at any altitude below the particle release height can result in errors in the magnitude of deposition density downwind. Furthermore, even when the actual meteorological conditions at

the test site were in agreement with the meteorological input data used by the model, there is no guarantee that the model will predict correct depositions because the meteorology downwind can also be in error.

Significant differences in predicted fallout were frequently observed when precipitation processing was enabled as compared to when precipitation processing was disabled. As shown in Table 2, the differences in deposition were occasionally as great as a factor of three, although generally much less. Often, the amount of fallout was reduced at a given atoll when precipitation processing was enabled, apparently due to cloud depletion at upwind locations. At other times, predicted deposition was higher, suggesting local rainout or washout. The limitations in the HYSPLIT wet deposition model (in common with other meteorological models), and the lack of precipitation data on an event-specific basis, may have contributed, in some cases, to the quantitative differences seen between the measured fallout deposition and model simulated estimates at some locations at some times.

Based on comparisons for tests where significant monitoring data were available, predicted depositions using the HYSPLIT three-dimensional particle model coupled with NCEP/NCAR reanalysis meteorological data agree with measured ^{137}Cs densities to within a factor of ten. This was almost always true when the initial wind speed and direction of the meteorological input data agreed reasonably well with that of the actual wind data at the test site.

Table 2. Comparison of HYPSLIT simulations of ^{137}Cs deposition density (Bq m^{-2}) with and without wet deposition for selected tests and atolls.

	Wet deposition disabled		Wet deposition enabled	
Atoll/Test	Atoll domain	1 degree domain	Atoll domain	1 degree domain
Fir (11 May 1958)[a]				
Kili	30	22	15	22
Ebon	30	30	40	22
Mejit	78	100	110	100
Flathead (11 June 1956)[a]				
Namorik	340	300	140	300
Wotho	5,200	3,300	4,100	3,000
Nectar (13 May 1954)[a]				
Namorik	40	160	85	160
Kili	74	40	48	40
Jabat	130	85	180	110
Lib	850	520	560	520
Lae	440	740	560	780
Dog (7 April 1951)[a]				
Kwajalein	5.2	3.3	9.3	6.7
Ujelang	24	110	60	190
Lae	0	2.6	3.0	5.6

[a] All dates GMT.

Inadequate meteorological data were generally the limiting factor in the HYSPLIT model's ability to predict accurate arrival times of fallout for Marshall Islands tests, although high-quality data on actual arrival times were also often lacking due to few measurements having been made and some inconsistencies between the available measurements (Beck et al. 2010). These conditions made comparing model-based estimates with measurements a difficult exercise. A comparison of model-predicted fallout arrival times with reported best estimates (Beck et al. 2010) is provided in Table 3.

As discussed, the HYSPLIT model uses a simple rainout and washout model that may not adequately simulate such complex processes, particularly for the relatively large amounts of debris in nuclear test clouds. For this reason and because of the normal high frequency of precipitation events in the Marshall Islands, most of which would not have been recorded in archival meteorological data sets, particularly in the southern atolls (Beck et al. 2010) where rainfall is the highest, the HYSPLIT simulations may not have predicted some actual deposition events. Moreover, it is possible that some of the differences in the HYSPLIT-predicted fallout arrival times as compared to the generally earlier arrival times observed could be a result of fallout deposited as a result of precipitation scavenging from unrecorded precipitation events.

Test-specific results. The results of simulations of fallout from five nuclear tests in the Marshall Islands are discussed here. Simulation results were compared against existing measurement data when possible, although anecdotal reports of fallout from test participants were considered as well. Further details on the characteristics and dates of the tests are given in an appendix of a companion paper (Beck et al. 2010).

Greenhouse Dog was a pure fission device which was detonated on Enewetak Atoll on 7 (GMT) April 1951. No radiological survey data are available for the Dog test. However, the HYSPLIT simulations suggest that small amounts of fallout could have occurred at several atolls in the Marshall Islands including Ujelang (Fig. 1), Wotho, Kwajalein, and Utrik. Model-predicted wind speed and direction agree fairly well with the observed values reported in DNA (1979) (Table 4). Dog is an example where HYSPLIT simulations were particularly valuable because there are no historical monitoring data.

Greenhouse Item was a fusion device detonated on Enewetak Atoll on 24 (GMT) May 1951. Similar to the situation for Dog, no radiological survey data exist for the Item test. The HYSPLIT simulation suggests there was significant fallout at Ujelang Atoll (Fig. 1). Because

Table 3. Comparisons of time of arrival (TOA) predicted by HYSPLIT with estimates based on measurements.

Test	Test date (GMT)	Test site	Distance to test site (km)	TOA: best estimate (h)	TOA: HYSPLIT estimate (h)	% difference
Bravo	28 Feb 1954	Rongelap	180	5.6	4.5	−20
		Ujelang	521	18	40	122
		Majuro	836	48	102	113
Romeo	26 Mar 1954	Rongelap	180	<30	97	223
		Kwajalein	426	100	104	4
		Majuro	836	100	118	18
Yankee	4 May 1954	Rongelap	180	<30	5	−83
		Kwajalein	426	35	154	340
		Utrik	486	30	105	250

the wind speed and direction used in the HYSPLIT simulation are in good agreement with data collected at the test site (Table 5), we assumed that significant fallout most likely did occur at Ujelang. A comparison of the total estimated ^{137}Cs deposition from tests after 1951 with soil sample data (Beck et al. 2010) also suggested that there was significant fallout at Ujelang Atoll from this test. The combination of empirical evidence and simulation supports the supposition that the missing fallout had to occur from either the Item or Dog test, or possibly both.

Castle Bravo, the largest U.S. test ever and the test that resulted in the largest individual exposures (Simon 1997), was a thermonuclear device detonated on 28 (GMT) February 1954 with a reported yield of 15 Mt. A considerable amount of monitoring data is available for the northern Marshall Islands for the Bravo test including data from fixed-wing aircraft as well as ground surveys of many atolls (Beck et al. 2010; Breslin and Cassidy 1955). In addition, gummed film (GF) data were collected at Kwajalein and Majuro Atolls; automatic continuous exposure rate monitors were also in operation at Majuro and Ujelang (Beck et al. 2010; Breslin and Cassidy 1955) during the Bravo test. Unfortunately, no GF data were available for Kwajalein covering the days immediately following the test; however, later data indicate that there was significant fallout several days afterwards, suggesting that additional fallout may have occurred at other atolls after the air monitoring had ceased. Since some of the atolls were surveyed only once by air at about 2 d after the test (Breslin and Cassidy 1955), there is also a strong possibility that additional fallout occurred after the surveys, particularly at Kwajalein, Wotho, and atolls south of Kwajalein. Daily GF measurements at Kwajalein and Majuro (Beck et al. 2010) often indicated that fallout persisted for many days after the air surveys were completed. The HYSPLIT simulations for Bravo proved useful in helping to interpolate fallout deposition over some of the southern atolls where the airplane monitoring data were either sparse or suspect because of known instrument problems. The model predicted significant fallout at Ujae and Lae contrary to survey data, although estimates at most other atolls agree within an order of magnitude (Fig. 2). The agreement between HYSPLIT and DNA (1979) wind data at the detonation site was poor at some altitudes (Table 6) suggesting a reason for the slight shift in the HYSPLIT-predicted fallout pattern compared to the observed pattern of deposition.

The Redwing Flathead test was detonated at Bikini Atoll on 11 (GMT) June 1956 with a reported total explosive yield of 356 kt of which, according to unofficial reports, was ~73% from fission. The pattern of HYSPLIT-predicted fallout for the Flathead test was generally consistent with the few available monitoring data. However, HYSPLIT-predicted ^{137}Cs deposition was about a factor of three higher than the GF measurement for Kwajalein and about a factor of twenty higher than the survey data for Wotho.

Test Fir, in the Hardtack I series, was a thermonuclear test which was detonated on Bikini Atoll on 11 (GMT) May 1958. Based on monitoring data at Utrik, Ujelang, Wotho, and Rongelap Atolls, as well as GF data at Kwajalein Atoll, only very light fallout occurred in the Marshall Islands from any of the 35 tests in 1958, including Fir. HYSPLIT simulations of other 1958 tests indicated that the Fir test was probably the most significant contributor to regional deposition during 1958. Model predictions for the Fir test indicated that most of the fallout occurred in areas to the east of the test site and that little fallout occurred south of Kwajalein, consistent with the available monitoring data. The estimated ^{137}Cs deposition agreed with ^{137}Cs deposition density monitoring data within a factor of three at Ujelang and Utrik and within a factor of 5 to 10 at the three other sites (Wotho, Kwajalein, and Rongelap).

Summary of Marshall Islands simulations. The availability of high quality three-dimensional and temporal meteorological data is a key factor for success in predicting the arrival time and location of fallout deposition. The comparisons presented here indicate the

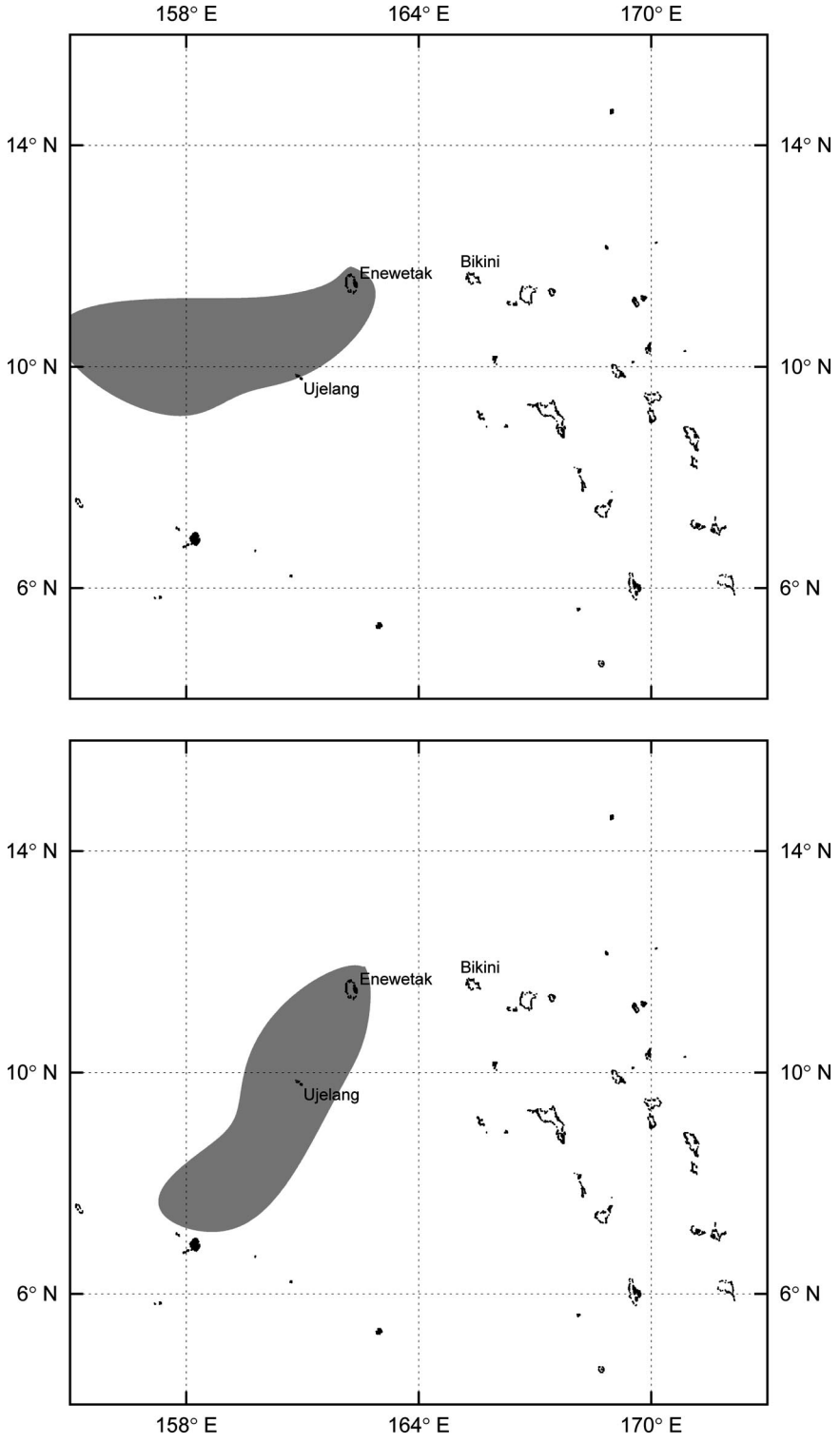

Fig. 1. Top Panel: HYSPLIT-predicted fallout pattern near Ujelang Atoll resulting from the Dog test. Bottom Panel: HYSPLIT-predicted fallout pattern at Ujelang Atoll resulting from the Item test.

importance of accurate upper-air wind data which largely influence the trajectory of the radioactive cap cloud that contains over 80% of the radioactivity. There were, however, only a few weather stations in the Marshall Islands during the years of nuclear testing (1946–1958) and they were located at significant distances from the nuclear weapons test sites. Thus, there were limited meteorological data collected that were directly relevant.

Table 4. Comparison of wind speed and direction at time of detonation at the Enewetak test site for the 7 April 1951 (GMT) Dog test.

	DNA (1979)		HYSPLIT	
Altitude (m)	Wind speed (km h^{-1})	Wind direction (deg)	Wind speed (km h^{-1})	Wind direction (deg)
1,524	48	80	45	81
3,048	35	80	27	57
4,572	38	70	21	35
6,096	35	30	19	22
7,620	19	300	19	134
9,144	50	280	23	298
10,668	47	230	37	266
12,192	53	220	45	259
13,716	42	280	45	262
15,240	35	310	32	275
16,764	50	340	19	288

Table 5. Comparison of wind speed and direction at time of detonation at the Enewetak test site for the 24 May 1951 (GMT) Item test.

	DNA (1979)		HYSPLIT	
Altitude (m)	Wind speed (km h^{-1})	Wind direction (deg)	Wind speed (km h^{-1})	Wind direction (deg)
1,524	26	90	21	103
3,048	8	90	16	114
4,572	14	260	11	50
6,096	14	290	13	2
7,620	19	250	19	147
9,144	16	360	23	352
10,668	14	250	18	318
12,192	13	280	13	280
13,716	—	—	11	278
15,240	—	—	11	310
16,764	—	—	11	345

Other sources of weather observations from this region are largely conjectural, but may have included data collected from passing ships at sea and aircraft. Comparisons with the actual wind data from the test site (DNA 1979) and the model-predicted wind data at the test site resulted in only sporadic agreement between the two. Furthermore, Kistler and Kalnay (2000) indicated that upper-air rawinsonde observations were inconsistent and very few in the tropics during this time period resulting in reanalysis forecasts of poor quality. For these various reasons, the meteorological input data used for HYSPLIT simulations, solely based on the NCAR/NCEP reanalysis model, did not often reproduce downwind meteorological conditions accurately enough to predict trajectories of the radioactive debris clouds with strong certainty. Despite these limitations, the simulations proved useful for indicating which tests could have impacted the Marshall Islands and which likely did not, particularly for years with no actual monitoring data (Beck et al. 2010). Simulations were also useful for interpolating between actual monitoring data for atolls that were not surveyed.

Nevada Test Site: Upshot-Knothole Harry

Upshot-Knothole Harry was a 32 kt fission device detonated on 19 May 1953 at the NTS. The Harry test was simulated using the HYSPLIT model with the purpose of comparing deposition patterns and fallout arrival times to published data (Beck et al. 1990; Beck and Anspaugh 1991) as well as with the meteorological modeling results of Cederwall and Peterson (1990).

Particle sizes and release heights for the Harry simulation closely followed those selected by Cederwall and Peterson (1990). Trajectory endpoint calculations and fallout pattern plots produced by Cederwall and Peterson (1990) indicated two diverging air masses at approximately H+10 h downwind. At lower altitudes, particles were shown to deposit at latitudes between the northern border of New Mexico and Denver, CO, while particles aloft deposited further to the south at latitudes between Cedar City, UT, and Albuquerque, NM. Using this information, two separate simulations were performed, each modeling the respective bottom and top halves of the debris cloud. The particle sizes used in the simulation ranged from 5 to 1,000 μm in diameter (Table 7).

Deposition parameters in our Harry simulations differed from those used by Cederwall and Peterson (1990). Cederwall and Peterson (1990) chose a fixed deposition velocity of 0.005 m s^{-1} to represent a range of values for various radionuclides and modeled only washout, not rainout, assuming that precipitation removed only airborne material below the radioactive debris cloud. As stated previously, in applying HYSPLIT, the deposition velocity was assumed to be only attributed to gravitational settling. Also, both below-cloud and in-cloud wet deposition processes were simulated. It should be noted that the model used by Cederwall and Peterson (1990) incorporated a washout coefficient dependent on precipitation rate; in contrast, in the HYSPLIT model, the rainout coefficient is dependent upon the precipitation rate and the washout coefficient is independent of it.

Results. The fallout patterns and fallout arrival times resulting from the Harry simulation agree reasonably well with those reported by Cederwall and Peterson (1990), but there are some noticeable differences. Fig. 3 shows that at H+12 h, the HYSPLIT-predicted debris cloud had entered Colorado and New Mexico and by H+18 h the debris cloud had reached Denver in the north and crossed into New Mexico much further south. The fallout pattern produced by HYSPLIT appears to agree with the estimated centerline of the plume produced by Cederwall and Peterson (1990). However, the patterns disagree in some locations. Cederwall and Peterson's pattern is broader north to south. Furthermore, the

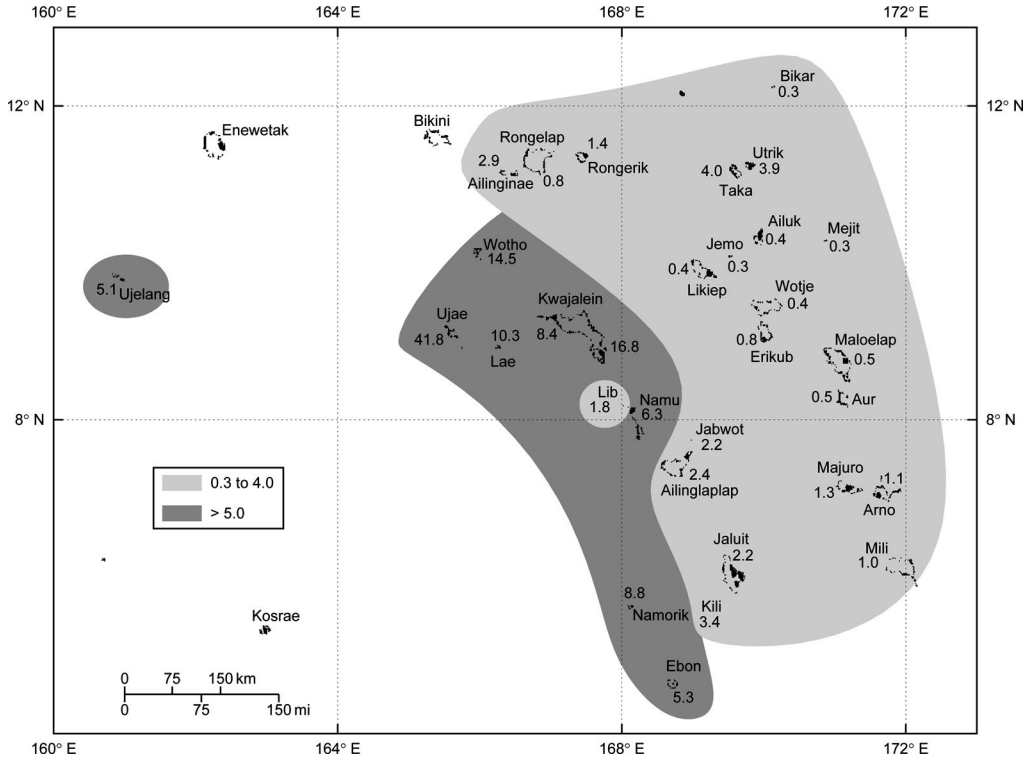

Fig. 2. Ratio of predicted ^{137}Cs deposition density (Bq m^{-2}) from simulations using the NOAA-HYSPLIT model and deposition density (Bq m^{-2}) inferred from available measurement data from the Bravo test.

Table 6. Comparison of wind speed and direction at time of detonation at the Bikini test site for the 28 February 1954 (GMT) Bravo test.

	DNA (1979)		HYSPLIT	
Altitude (m)	Wind speed (km h^{-1})	Wind direction (deg)	Wind speed (km h^{-1})	Wind direction (deg)
1,524	16	100	27	136
3,048	10	310	16	303
4,572	24	290	19	282
6,096	24	380	32	264
7,620	35	260	47	253
9,144	48	250	58	250
10,668	64	240	66	258
12,192	64	230	71	265
13,716	84	250	69	264
15,240	58	250	56	285
16,764	29	200	42	308
18,288	—	—	24	331
21,336	—	—	10	124
24,384	—	—	23	74
27,432	—	—	45	92
30,480	—	—	72	96

Table 7. Particle size distribution used for the Harry simulation.

Particle size range (μm)	Increment in range (μm)
5 to 50	5
60 to 100	10
125 to 300	25
350 to 700	50
800 to 1,000	100

deposition estimates do not agree well quantitatively. In general, HYSPLIT indicated that the more significant deposition occurred slightly north of the location reported in Cedarwall and Peterson (1990). For example, the HYSPLIT simulation indicated little fallout at St. George, UT, a location in which significant fallout is known to have occurred (Anspaugh and Church 1986; Beck and Anspaugh 1991). This difference is likely due to disagreements between the wind data at downwind grid locations used in our simulations as compared to the simulations of Cederwall and Peterson (1990). Cederwall and Peterson (1990) also reported that adjustments to certain fallout parameters in their model were needed to create an agreement between simulation results and measurement data.

Semipalatinsk Nuclear Test Site: Test #1

The first Soviet nuclear detonation took place on 29 August 1949 with a yield of 22 kt. This detonation was a surface burst at the Semipalatinsk Test Site in Kazakhstan. The test is believed to have been identical in construction to the first U.S. nuclear test, Trinity (Rhodes 1986), conducted in New Mexico in 1945. The maximum cloud height was ~9 km. At the time of the test, there

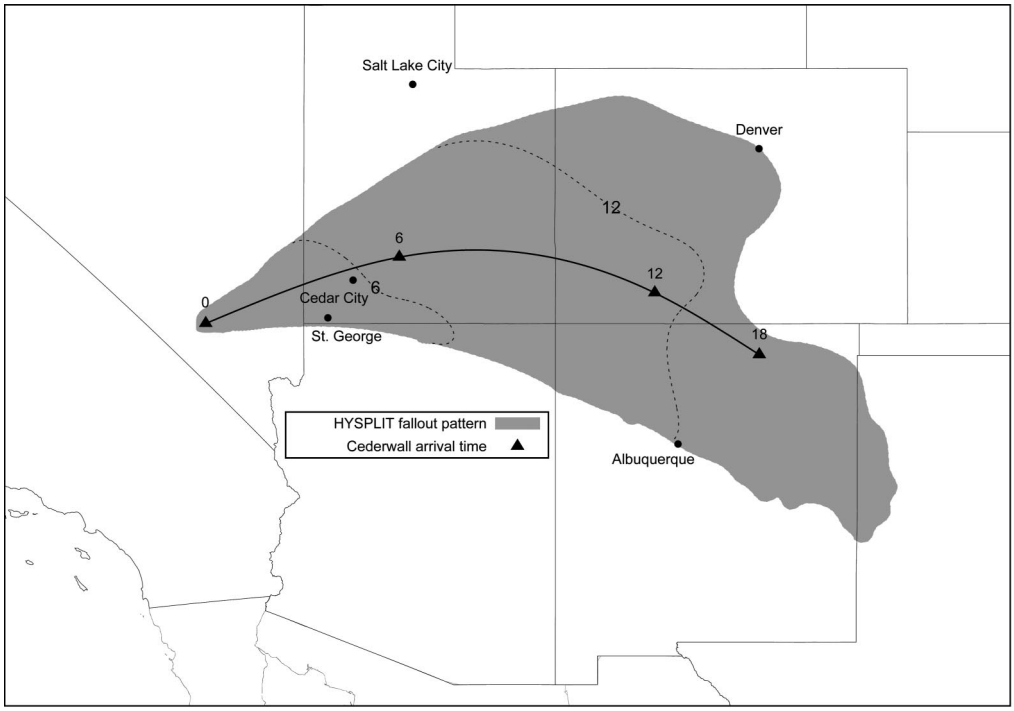

Fig. 3. HYSPLIT fallout pattern resulting from simulations of the Upshot-Knothole Harry test. The solid black line indicates the estimated centerline of the radioactive cloud as simulated by Cederwall and Peterson (1990). Dashed lines delineate the HYSPLIT predictions of the geographic boundary of the fallout pattern at the time noted.

were strong northeasterly winds estimated at 47–60 km h^{-1} with almost no wind shear (Shoikhet et al. 1998; Imanaka et al. 2005).

HYSPLIT simulations were performed to compare predicted estimates of ^{137}Cs deposition density with published estimates of the fallout pattern and the spatial distribution of ^{137}Cs and ^{239,240}Pu near the village of Dolon, Kazakhstan. Fallout was reported to have reached Dolon, approximately 118 km northeast of ground zero, at roughly H+2 h (Yamamoto et al. 2008; Gordeev et al. 2002). Soil samples were collected in 2005 by Yamamoto et al. (2008) at 21 locations along a line approximately perpendicular to the supposed centerline of the plume. Their analyses of ^{137}Cs and ^{239,240}Pu suggested that (1) the spatial distribution of ^{137}Cs and ^{239,240}Pu is roughly Gaussian in shape and perpendicular to the axis of the fallout trajectory with maximums located near the supposed axis-center, and (2) the width of the fallout pattern near Dolon was approximately 8–10 km (Yamamoto et al. 2008).

To calculate the fallout deposition at locations downwind, particle releases at varying altitudes were simulated using HYSPLIT. The total number of particles in the simulated debris cloud was apportioned using the estimated total ^{137}Cs activity, particle size, and spatial distribution model described previously for the Marshall Islands simulations as well as the alternate distributions given in Table 1. The release heights in the simulation ranged from 450 m AGL to the reported maximum cloud height, ~9 km, and are shown in Table 8. The cloud bottom, estimated at 2.7 km, was based on the reported cloud dimensions of the Trinity test. The assumed particle sizes varied from 5 μm up to 300 μm, in 5 μm increments, depending on the activity distribution, and the simulation was carried out to 5 h post-detonation. The total number of particles tracked in different simulations varied from 1×10^7 to 2.5×10^7.

Results. The calculated ^{137}Cs deposition pattern for the first Soviet nuclear detonation, using the MI ^{137}Cs activity-size distribution from Table 1, is shown in Fig. 4. The simulation data were gridded at a resolution of ~4.3 km^2. Sites A, B, and C in Fig. 4 correspond to the

Table 8. Particle release heights and fraction of total ^{137}Cs activity corresponding to each release height for the first test at the Semipalatinsk Nuclear Test Site.

Release height (m AGL)	Height increment (m AGL)	Fraction of total ^{137}Cs activity
450 to 2,700	450	0.12
2,875 to 3,750	175	0.10
3,925 to 4,800	175	0.16
5,150 to 6,900	350	0.36
7,075 to 7,950	175	0.16
8,125 to 9,000	175	0.10

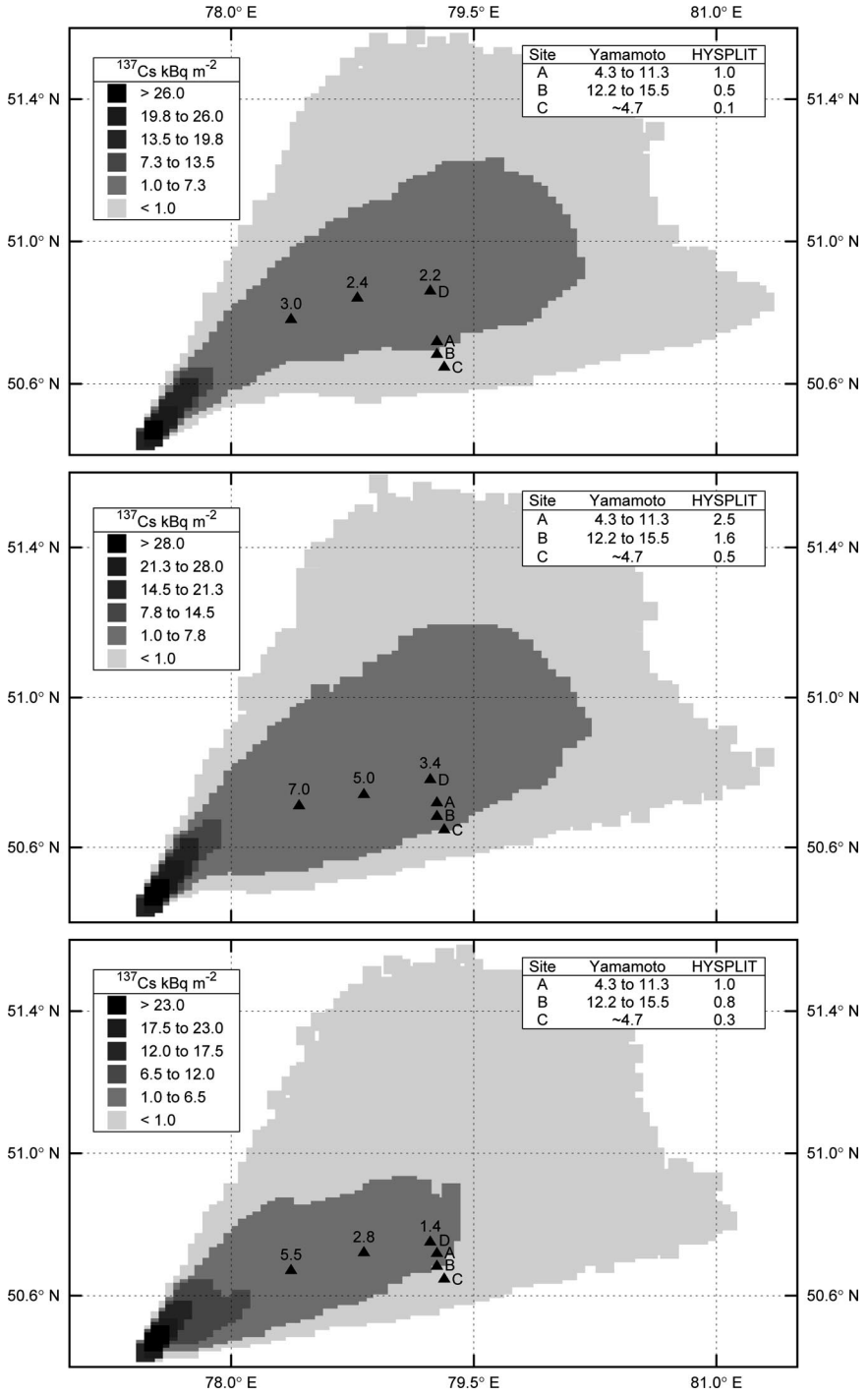

Fig. 4. HYSPLIT predictions of ^{137}Cs deposition pattern near the Semipalatinsk Test Site in Kazakhstan following event 1 (29 August 1949) using: MI particle-size distribution (Top Panel), alternate particle-size distribution #1 (Center Panel), and alternate particle-size distribution #2 (Bottom Panel), all described in Table 1. The key in each panel compares simulation results and measurements reported by Yamamoto et al. (2008).

Yamamoto et al. (2008) sampling locations. Location D is the grid cell with the highest HYSPLIT-predicted deposition density at ~118 km downwind. Sites A and C are the respective northern and southern-most sites listed in the Yamamoto et al. (2008) study. The predicted fallout arrival time at Dolon is reasonably consistent with that reported by Gordeev et al. (2002) and Yamamoto et al. (2008) at approximately 2 to 3 h, but the spatial distribution of ^{137}Cs is much wider than that inferred by the measurements of Yamamoto et al. (2008), and the

direction of the ^{137}Cs deposition pattern is significantly further to the north than the Yamamoto et al. (2008) data. However, the deposition patterns resulting from the alternative ^{137}Cs activity-size distributions given in Table 1 (Fig. 4) shift the HYSPLIT fallout pattern closer to that reported in Yamamoto et al. (2008) and clearly indicate that the predicted ^{137}Cs deposition is very sensitive to the estimated fraction of ^{137}Cs on particles greater than 50 μm. As discussed earlier, and shown in Table 1, the distribution used for the Marshall Islands simulations assumed only about 20% of the ^{137}Cs activity on particles greater than 50 μm, while the alternate distributions assume a larger fraction of ^{137}Cs on particles of diameter greater than 50 μm. As shown in Fig. 5, where the activity on various size groups of particles is plotted separately, the HYSPLIT simulation indicates that most of the particles depositing in the vicinity of Dolon, and particularly along the axis of the fallout pattern, to be greater than 50 μm in diameter, while the particles further from the centerline were generally less than 50 μm. However, even assuming a greater fraction of ^{137}Cs activity on large particles, the HYSPLIT pattern still deviates from the axis of the Yamamoto data and is much broader, presumably reflecting the wind shear present in the meteorological input data. HYSPLIT air mass trajectories (Fig. 6) clearly illustrate the significant wind shear, which is inconsistent with the assertion that wind shear was minimal (Shoikhet et al. 1998; Imanaka et al. 2005).

Although the estimated peak ^{137}Cs deposition density predicted by HYSPLIT in the vicinity of Dolon (Table 9) is slightly closer to that measured by Yamamoto et al. (2008) (corrected for decay) for the alternative particle-size distributions than for the MI distribution, the HYSPLIT maximum deposition density near Dolon is still much lower than the maximum measured by Yamamoto et al. (2008) (corrected for decay). However, this is to be expected since, as a result of the predicted wind shear, the HYSPLIT fallout is spread over a wider area compared to the Yamamoto et al. (2008) soil data and, thus, is diluted.

We surmise the shift of the HYSPLIT pattern to the north, compared to the measurements of Yamamoto et al. (2008), to be a result of wind shear in our meteorological data and other limitations of those data. However, it may also partly reflect the fact that the ^{137}Cs activity-size model used in HYSPLIT simulations is too crude and may not be apportioned to give enough of the total ^{137}Cs activity on the larger particles that deposit closer to the

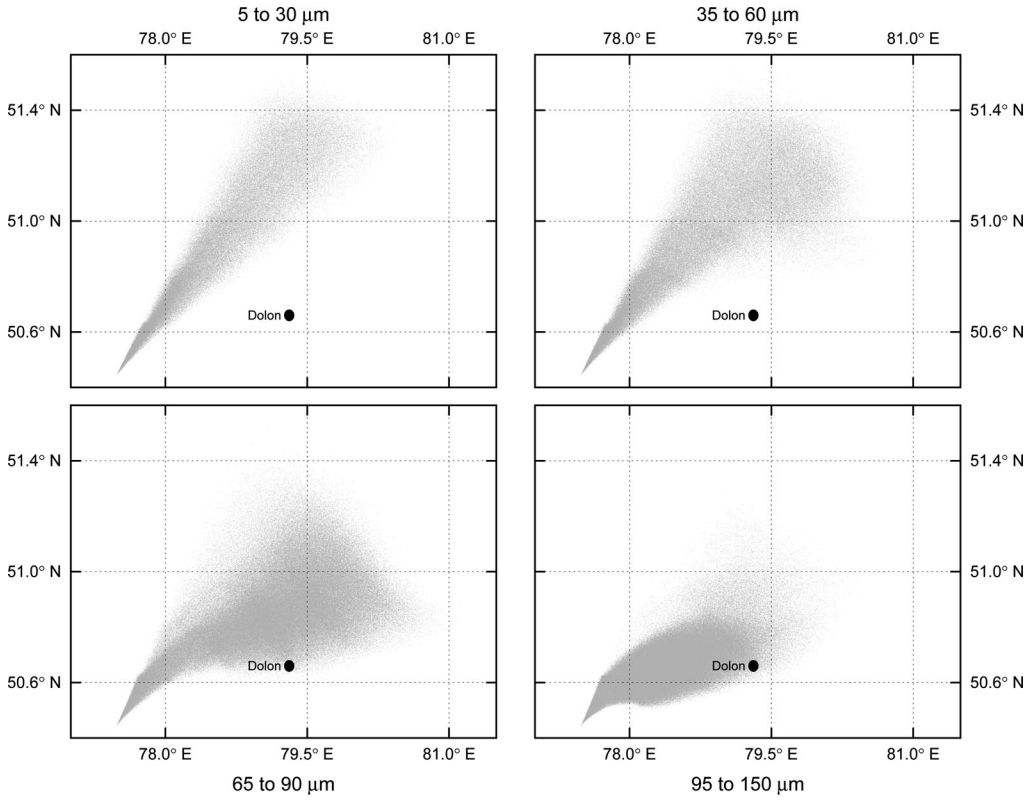

Fig. 5. HYSPLIT-predicted fallout patterns of different particle sizes at the Semipalatinsk Test Site in Kazakhstan following event 1 (29 August 1949).

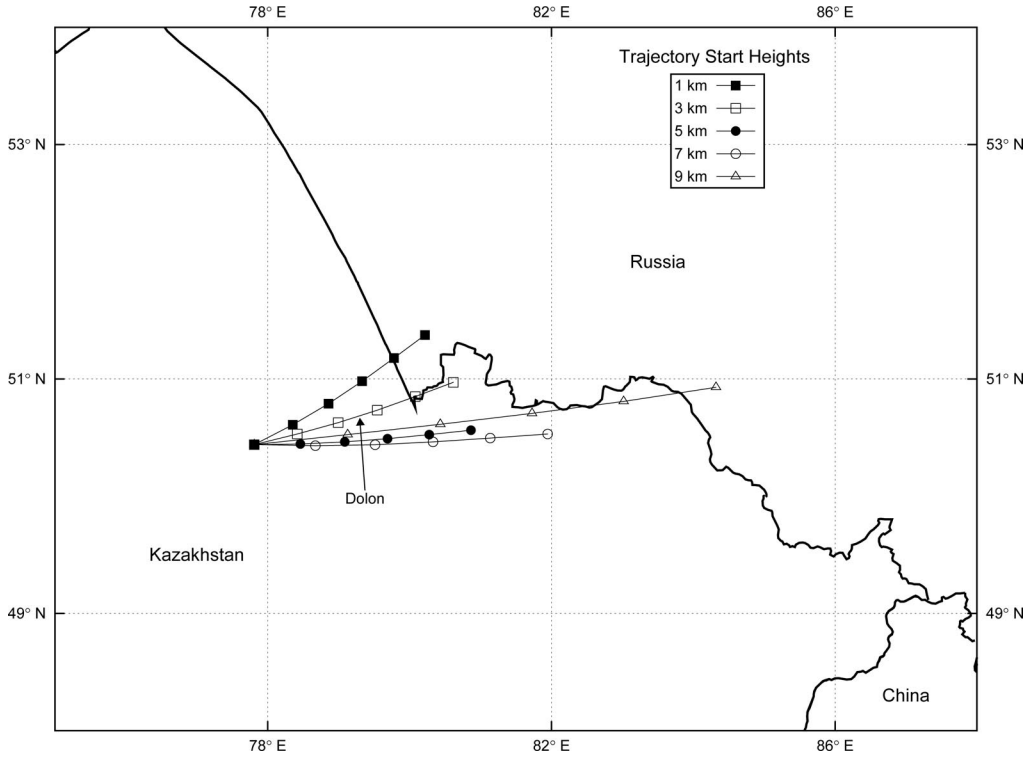

Fig. 6. HYPSLIT air mass trajectories illustrating wind shear derived from archival meteorological data that were inconsistent with reported actual weather conditions at the Semipalatinsk Test Site at time of detonation. Symbols are plotted in 1 h intervals. The wind shear resulted in different sized particles depositing in the vicinity of Dolon over a wider area (Fig. 5) than indicated by retrospective soil sample analyses.

Table 9. Comparison of HYSPLIT predicted peak ^{137}Cs deposition density using three different particle size distributions with decay corrected measurements of Yamamoto et al. (2008).

Distribution	HYSPLIT-predicted maximum (kBq m^{-2})	HYSPLIT prediction at location of Yamamoto et al. (2008) axis (kBq m^{-2})	Measurements of ^{137}Cs from Yamamoto et al. (2008) at axis (kBq m^{-2})	Ratio: Yamamoto data to HYSPLIT
MI (from Table 1)	2.2	0.5	12–16	24 to 32
Alternate #1	3.4	1.6	12–16	7 to 10
Alternate #2	1.4	0.8	12–16	15 to 20

centerline of the Yamamoto et al. (2008) pattern. This could account for a broadening of our predictions. It should also be noted, however, that the Yamamoto et al. (2008) soil sample data were obtained almost a half century after the test and may not accurately reflect the original deposition pattern because of weathering and redistribution. The Yamamoto measurement data exhibit significant scatter and many of the samples were taken over bare soil where those processes could have been particularly important. This is particularly true for the samples taken in Dolon itself. Thus, the true width of the original ^{137}Cs deposition pattern may lie somewhere between that predicted by the contemporary soil measurements and that predicted by the HYSPLIT model.

The HYSPLIT simulations reflect, at least, the same order of magnitude of the peak ^{137}Cs deposition density in the vicinity of Dolon, taking into account the dilution of the HYSPLIT maximum deposition density as a result of the additional dispersion of the fallout about the axis. They also illustrate the impact of fractionation on the relative deposition density of volatile nuclides such as ^{137}Cs (i.e., deposition of small particles) compared to refractory elements such as ^{239,240}Pu (i.e., deposition of large particles). As illustrated in Yamamoto et al. (2008), the soil data clearly show a different dispersion (pattern width) about the fallout pattern centerline for ^{239,240}Pu as opposed to ^{137}Cs, as expected since the ^{239,240}Pu is mostly on large particles. The pattern of particle size and ^{137}Cs deposition indicated by the HYSPLIT model is qualitatively consistent with that expected from highly fractionated local fallout (see companion paper by Ibrahim et al. 2010).

APPLICATION OF HYSPLIT TO MARSHALL ISLANDS FALLOUT ASSESSMENT

HYSPLIT model simulations were used to support the analysis of deposition of fallout in the Marshall Islands and related dose assessments (Beck et al. 2010; Bouville et al. 2010; Simon et al. 2010a, 2010b). This application is described below.

Simulations of air mass trajectories and deposition patterns were used to help make ^{137}Cs deposition density estimates for specific locations in the Marshall Islands for tests in which fallout monitoring data were either sparse or nonexistent. The results were used to assist in interpolations of deposition at atolls where no monitoring data were available using measurements of deposition at nearby atolls (Beck et al. 2010).

Despite the uncertainty found after testing the model under conditions of questionable input data and limited measurement data, the model-based deposition estimates were useful in estimating fallout deposited in the Marshall Islands (Beck et al. 2010) in certain specific cases. For example, the HYSPLIT predictions were the only source of information on fallout deposited and often supported anecdotal reports of significant fallout prior to 1952 when there were no monitoring data. This is particularly true at Ujelang Atoll where anecdotal reports indicated fallout resulting from the 1951 Greenhouse Dog and Item tests but no actual measurements were reported. Additionally, the HYSPLIT model simulations were used to support interpolations of deposition and time of arrival, and to fill out the estimated deposition patterns from the 1956 and 1958 tests for which only a few (4 to 6) atolls were monitored. For example, for the 1956 Flathead test, model predictions were used in conjunction with GF measurements at Kwajalein and survey measurements at Ujelang, Wotho, Rongelap, and Utrik, to estimate fallout at atolls south and east of Kwajalein where no actual measurements were made. Only very low levels of fallout deposition were predicted in other areas. Similarly, for the 1958 Fir test, the HYSPLIT simulations were used to aid in estimating the relatively low levels of deposition at atolls not monitored. As discussed in Beck et al. (2010), a high uncertainty estimate (a probability distribution function with a geometric standard deviation of 3.0) was applied to the HYSPLIT-based deposition density estimates.

Although uncertain, the HYSPLIT results had relatively little impact on estimates of total fallout in the Marshall Islands presented in Beck et al. (2010) because the model-predicted fallout estimates used were almost always small compared to fallout levels from tests with monitoring data. This was the case, for example, for the 1956 and 1958 tests compared to the 1954 Castle tests. For this reason, the uncertainty contribution of the HYSPLIT simulations to the overall uncertainty of the estimated external and internal doses (Bouville et al. 2010; Simon et al. 2010a) was also small.

CONCLUSION

A well-established meteorological model, HYSPLIT, was tested for its ability to predict dispersion and deposition of nuclear test-related fallout at varying distances downwind. The model was evaluated by comparing model-predicted deposition patterns and arrival times against measured deposition density. Particles of varying sizes were released from a range of starting heights to represent a stabilized radioactive debris cloud. Deposition domains were defined to track the locations of deposited particles so as to test the model's ability to predict downwind depositions of differently sized particles at specific locations in agreement with known patterns.

Because of the general limited availability of ground-based radiological measurement data, it is very difficult to separate the relative contributions of different factors to the overall predictive ability of HYSPLIT. Results from our simulations suggest that the accuracy and spatial resolution of the meteorological input data is one of the most important factors in modeling fallout with the HYSPLIT model since the advection and dispersion calculations directly depend on the meteorological data. The simplification of physical processes and the particle distribution that is assumed in the debris cloud model, as well as in the wet deposition model implemented in HYSPLIT, all may have had an impact on the quantitative predictions of fallout at a particular atoll. When relatively accurate wind data were used, however, we confirmed that the model-predicted deposition is reasonably consistent with available ground measurement data.

In our simulations, meteorological reanalysis data were used. Although methods in data assimilation and reanalysis have greatly improved, reanalyses prior to the geophysical year (1957–1958) still suffer from a lack of satisfactory observations. However, the HYSPLIT model was able to predict reasonably accurate fallout arrival times for simulations in which the meteorological reanalysis data were consistent with observed data at several altitudes within the cap of the stabilized debris cloud at the test site. Under those conditions, model-predicted arrival times were often within several hours of those reported. Conversely, when the reanalysis data did not agree with the local observed wind measurements, fallout arrival times and depositions deviated, largely in some cases, from reported values in the literature.

The type of meteorological data provided by most reanalysis models makes it difficult to model wet deposition. Atmospheric models may incorporate simplifying assumptions for wet deposition, as does the HYSPLIT model, or may disregard the wet removal process altogether. Wet deposition can be a large contributor to fallout under conditions of precipitation and can often lead to localized pockets of elevated radioactivity. Thus, to accurately model fallout through computer simulation, a refined wet deposition model would be needed in conjunction with accurate precipitation data.

The assessment of fallout deposition in the Marshall Islands discussed in a companion paper (Beck et al. 2010) is a good example of retrospective modeling of the dispersion and deposition of fallout using the HYSPLIT model. HYSPLIT predictions of fallout deposition can be used for supplementing existing ground-based fallout measurement data, particularly when no ground-based fallout measurement data are available. In such cases, HYSPLIT can be used to indicate whether or not fallout might have occurred at a particular location and provide, at minimum, crude estimates of the magnitude of the deposited activity. This, in itself, can be a very valuable asset for the reconstruction of past fallout events.

Acknowledgments—This work was supported by the Intra-Agency agreement between the National Institute of Allergy and Infectious Diseases and the National Cancer Institute, NIAID agreement #Y2-Al-5077 and NCI agreement #Y3-CO-5117. The authors are indebted to Roland Draxler and Barbara Stunder of the NOAA Air Resources Laboratory in Silver Spring, MD, for their willingness and generosity in providing instruction and information about the operation and theory of the HYSPLIT model (http://ready.arl.noaa.gov/HYSPLIT.php).

REFERENCES

Anspaugh L, Church B. Historical estimates of external exposure and collective external exposure from testing at the Nevada Test Site through Hardtack II, 1958. Health Phys 52:35–51; 1986.

Beck HL, Anspaugh LR. Development of the county database: estimates of exposure rates and times of arrival of fallout in the ORERP Phase-2 area. Washington, DC: U.S. Department of Energy; DOE/NV-320; 1991.

Beck HL, Helfer IK, Bouville A, Dreicer M. Estimates of fallout in the western U.S. from Nevada weapons testing based on gummed-film monitoring data. Health Phys 59:565–570; 1990.

Beck HL, Bouville A, Moroz BE, Simon SL. Fallout deposition in the Marshall Islands from Bikini and Enewetak nuclear weapons tests. Health Phys 99:124–142; 2010.

Bouville A, Beck HL, Simon SL. Doses from external radiation to Marshall Islanders from Bikini and Enewetak nuclear weapons tests. Health Phys 99:143–156; 2010.

Breslin AJ, Cassidy ME. Radioactive debris from Operation Castle, islands of the mid-Pacific. Washington, DC: U.S. Atomic Energy Commission; 1955.

Cederwall RT, Peterson KR. Meteorological modeling of arrival and deposition of fallout at intermediate distances downwind of the Nevada Test Site. Health Phys 59:593–601; 1990.

Crocker G, O'Connor J, Freiling E. Physical and radiochemical properties of fallout particles. San Francisco, CA: U.S. Naval Radiological Defense Laboratory; Report USNRDL-TR-899; 1965.

Defense Nuclear Agency. Compilation of local fallout data from test detonations 1946–1962 extracted from DASA 1251. Washington, DC: DNA; DNA 1251-2-EX; 1979.

Draxler RR. HYSPLIT4 user's guide. Silver Spring, MD: National Oceanic and Atmospheric Administration; ERL ARL-230; 1999.

Draxler RR, Hess GD. Description of the hysplit4 modeling system. Silver Spring, MD: National Oceanic and Atmospheric Administration; ERL ARL-224; 1997.

Draxler RR, Hess GD. An overview of the hysplit4 modeling system for trajectories, dispersions, and deposition. Australian Meteorological Magazine 47:295–308; 1998.

Freiling EC, Crocker GR, Adams CE. Nuclear debris formation. In: Radioactive fallout from nuclear weapons tests. Proceedings of an USAEC Conference. Washington, DC: U.S. Atomic Energy Commission; 1965: 1–41.

Gordeev K, Vasilenko I, Lebedev A, Bouville A, Luckyanov N, Simon SL, Stepanov Y, Shinkarev S. Fallout from nuclear tests: dosimetry in Kazakhstan. Radiat Environmental Biophys 41:61–67; 2002.

Heidt WB, Schuert EA, Perkins WW, Stetson RL. Nature, intensity, and distribution of fallout from MIKE shot. San Francisco, CA: U.S. Naval Radiological Defense Laboratory; Report WT-615; 1953.

Hoecker WH, Machta L. Meteorological modeling of radioiodine transport and deposition within the continental United States. Health Phys 59:603–619; 1990.

Ibrahim SA, Simon SL, Bouville A, Melo D, Beck HL. Alimentary tract absorption (f_1 values) for radionuclides in local and regional fallout nuclear tests. Health Phys 99:233–251; 2010.

Imanaka T, Fukutani S, Yamamoto M, Sakaguchi A, Hoshi M. Width and center-axis location of the radioactive plume that passed over Dolon and nearby villages on the occasion of the first USSR A-bomb test in 1949. Radiat Res 46:395–399; 2005.

Izrael YA. Radioactive fallout after nuclear explosions and accidents. In: Baxter MS, ed. Radioactivity in the environment (vol. 3). Oxford, UK: Elsevier Science Ltd.; 2002.

Kalnay E, Kanamitsu M, Kistler R, Collins W, Deaven D, Gandin L, Iredell M, Saha S, White G, Wollen J, Zhu Y, Leetmaa A, Reynolds R, Chelliah M, Ebisuzaki W, Higgins W, Janowiak J, Mo KC, Ropelewski C, Wang J, Jenne R, Joseph D. The NCEP/NCAR 40-year reanalysis project. Bulletin American Meteorological Society 77:437–471; 1996.

Kinser AM. Simulating wet deposition of radiocesium from the Chernobyl accident. Columbus, OH: Air Force Institute of Technology Wright-Patterson Air Force Base; 2001. Thesis.

Kistler R, Kalnay E. The NCEP/NCAR reanalysis prior to 1958. In: Proceedings of the second World Climate Research Programme international conference on reanalysis. London: World Meteorological Organization; 2000: 27–35.

Klug W, Graziani G, Gridppa G, Pierce D, Tassone C. Evaluation of long range atmospheric transport models using envrionmental radioactivity data from the Chernobyl accident (The ATMES report). Essex, England: Elsevier Science Publishers; 1992.

National Cancer Institute. Estimated exposures and thyroid doses received by the American people from Iodine-131 in fallout following Nevada atmospheric nuclear bomb tests: a report from the National Cancer Institute. Washington, DC: Department of Health and Human Services; 1997.

Rhodes R. The making of the atomic bomb. New York: Simon and Schuster, Inc.; 1986.

Rowland R. Fallout computer codes: a bibliographic perspective. Washington, DC: U.S. Defense Nuclear Agency; DASIAC-SR-93-022; 1994.

Shoikhet YN, Kiselev VI, Loborev VM, Sudakov VV, Algazin AI, Demin VF, Lagutin AA. The 29 August 1949 nuclear test. Radioactive impact on the Altai region population. Barnaul, Russian Federation: Institute of Regional Medico-Ecological Problems (IRMEP); 1998.

Simon SL. A brief history of people and events related to atomic weapons testing in the Marshall Islands. Health Phys 73:5–20; 1997.

Simon SL, Bouville A, Land CE, Beck HL. Radiation doses and cancer risks in the Marshall Islands associated with exposure to radioactive fallout from Bikini and Enewetak nuclear weapons tests: summary. Health Phys 99:105–123; 2010a.

Simon SL, Bouville A, Melo D, Beck HL, Weinstock RM. Acute and chronic intakes of fallout radionuclides by Marshallese from nuclear weapons testing at Bikini and Enewetak and related internal radiation doses. Health Phys 99:157–200; 2010b.

Swanberg EL, Hoffert SG. Using atmospheric ^{137}Cs measurements and HYSPLIT to confirm Chernobyl as a source of ^{137}Cs in Europe. In: 23rd Seismic Research Review: Worldwide Monitoring of Nuclear Explosions. Los Alamos, NM: Los Alamos National Laboratory; 2001: 64–70.

Toon OB, Turco RP, Robock A, Bardeen C, Oman L, Stenchikov GL. Atmospheric effects and societal consequences of regional scale nuclear conflicts and acts of individual nuclear terrorism. Atmospheric Chem Phys 7:1973–2002; 2007.

Yamamoto M, Tomita J, Sakaguchi A, Imanaka T, Fukutani S, Endo S, Tanaka K, Hoshi M, Busev BI, Apsalikov AN. Spatial distribution of soil contamination by ^{137}Cs and ^{239,240}Pu in the village of Dolon near the Semipalatinsk Nuclear Test Site: new information on traces of the radioactive plume from the 29 August 1949 nuclear test. Health Phys 94:328–337; 2008.

■ ■